

## Response to Editorial Review

Dear editor:

Thank you very much for handling our manuscript. We really appreciate the insightful comments and suggestions from you and the reviewer. Below, we address the comments point-by-point, and the comments are italicized and our response follow in blue.

Major points

*Comment 1: As has been raised before, I think some discussion is necessary as to whether it is not to be expected that there is such a correlation as  $U$  and  $R$  are derived from NEP.*

Response: Thanks for this suggestion. As shown in Figure 2, this method was applied on the atmospheric inversion product. However, some ecosystems seem to defy such correlation. Therefore, we think the robustness in relationship between annual NEP and  $U/R$  depend on the stability of carbon uptake sensitivity for an ecosystem. We have added discussions as (Lines 297-303): “In this study, the atmospheric inversion product shows low correlation between NEP and  $\ln\left(\frac{U}{R}\right)$  in some boreal ecosystems, which might due to that the atmospheric inversion product is failed to capture the carbon uptake sensitivity in these boreal ecosystems or these boreal ecosystems are experiencing serious disturbances. Therefore, the robustness in relationship between annual NEP and  $\ln\left(\frac{U}{R}\right)$  depends on the temporal stability of carbon uptake sensitivity for an ecosystem. In addition, the spatial variation in  $\beta$  reveals the differences of carbon uptake sensitivity across ecosystems”.

*Comment 2: Please provide a derivation of Eq 4. This does not logically follow from Eq. 1*

Response: Thanks for this suggestion. To avoid logic misleading, we have deleted Eq.1. In addition, we have added some sentences to illustrate the motivation of testing the relationship between annual NEP and the ratio  $U/R$  (Lines 159-167): “Many studies have reported that the vegetation net  $\text{CO}_2$  uptake during the growing season and the non-growing season soil net  $\text{CO}_2$  release are tightly correlated (Luo et al., 2014; Zhao et al., 2016). Therefore, we further tested the relationship between annual NEP and  $\frac{U}{R}$  (i.e.,  $NEP \propto \frac{U}{R}$ ), which reflects the seasonal carbon uptake-release ratio. Consequently, NEP in any given ecosystem can be expressed as (Fig. S2):

$$NEP = \beta \cdot \ln\left(\frac{U}{R}\right) \quad (3)$$

where the parameter  $\beta$  represents the slope of the linear relationship of  $NEP \propto \ln\left(\frac{U}{R}\right)$ , indicating the site-level carbon uptake sensitivity”.

Minor points

*L41 rephrase to “large-scale estimates from an atmospheric inversion product”*

Response: Thanks, done as suggested.

*L44: linearly related to  $\ln(X)$  is equivalent to logarithmically related to  $X$ ?*

Response: Thanks, and we have rephrased this sentence as “NEP could be logarithmically indicated by U/R”.

*L45: beta has not been defined (the slope of what?). Explain “well indicated”*

Response: Thanks, and we have rephrased this sentence as “while the spatial distribution of  $I_{AV_{NEP}}$  was associated with the slope (i.e.,  $\beta$ ) of the logarithmic correlation between annual NEP and U/R”.

*L49: gridded products of what?*

Response: Thanks, and we have revised it as “gridded NEP products”.

*L77: unclear what “the compiled” refers to here*

Response: Thanks, and we have revised it as “the global flux tower-based product”.

*L82: Isn't this a contradiction? If they are strongly correlated in space, then how would they determine the spatial variation in NEP?*

Response: We have rephrased this sentence as (Lines 72-75): “The NEP in terrestrial ecosystems is determined by two components, including vegetation photosynthesis and ecosystem respiration (Reichstein et al., 2005), and their relative difference could determine the spatial variation of NEP (Baldocchi et al., 2015; Biederman et al., 2016)”.

*L107: here and in the following: the total NET uptake. Also this isn't entirely correct because as you note later also the strength of the source/sink within each period can vary.*

Response: Thanks for this suggestion. We have rephrased the description as “the total net CO<sub>2</sub> uptake flux (U)” and “the total net CO<sub>2</sub> release flux (R)” in the whole paper.

*L110: I don't understand the use of the word “innovatively attributed” here. Please clarify*

Response: We have rephrased it as “The variations of NEP thus could be attributed to these decomposed components”.

*L146: Add “to infer the net CO2 exchanges between land, ocean and atmosphere at large scales*

Response: Done as suggested.

*L165ff: Is this correct? Are the effects of land cover changes not implicitly included by the use of satellite derived fAPAR?*

Response: Thanks. We have revised the description of FLUXCOM product as ( Lines 140-144): “It should be noted that the inter-annual variability of FLUXCOM product is driven by meteorological measurements and satellite data, which partially includes information on vegetation state and other land surface properties”.

*L168: Please provide correct link to the data portal*

Response: Thanks. We have revised the link of FLUXCOM product.

*L190: A quantitative definition of CUP and CRP is missing here.*

Response: Thanks. We have added the definition of CUP and CRP as “where *CUP* ( $\text{d yr}^{-1}$ ) is the length of CO<sub>2</sub> uptake period and *CRP* ( $\text{d yr}^{-1}$ ) is the length of CO<sub>2</sub> release period”.

*L254: Verified is the wrong word here*

Response: We have revised it as “confirmed”.

*L272: use “across-site variation” instead to spatial change?*

Response: Done as suggested.

*L283: The use of “mostly” is inappropriate here, because CUP/CRP explains less than 60% of the variance.*

Response: We have rephrased it as “Therefore, the spatial distribution of mean annual NEP was more strongly driven by the phenological changes”.

*L317: But what if most of this crop IAV is related to changes in the local crop from year to year and are therefore not representative of regional scale cropland IAV?*

Response: Sorry for the confusion. We have rephrased this sentence as (Lines 247-249): “The highest  $\beta$  implies that the land covered by cropland with the largest  $\text{IAV}_{\text{NEP}}$ . Therefore, the reported rapid global expansion of cropland may enlarge the fluctuations in Land-atmosphere CO<sub>2</sub> exchange”.

*L325/L326: These statements need to be adjusted to reflect that the difference in explanatory power is “only” 58 to 42%.*

Response: Thanks for this suggestion.

First, we have rephrased the subtitle as “Joint control of plant phenology and physiology on mean annual NEP”.

Second, we have revised these sentences to emphasize the equal importance of plant phenology and physiology in driving the spatial difference of mean annual NEP as (Lines 255-257): “Here we demonstrated that the spatial difference of mean annual NEP

was determined by both the phenology indicator  $\frac{\text{CUP}}{\text{CRP}}$  (58%) and the physiological

indicator  $\frac{\bar{U}}{\bar{R}}$  (42%). In addition, the lower contribution of the physiological indicator could partly be attributed to the convergence of  $\frac{\bar{U}}{\bar{R}}$  across FLUXNET sites (Fig. S4)".

## Response to comments from reviewer #1

Comment 1: *The manuscript proposed to study the relationship between  $\ln(U/R)$  and NEP. Since we know that  $NEP = U - R$  and  $\ln(U/R) = \ln(U) - \ln(R)$ , therefore it is expected to see a strong  $r^2$  between  $\ln(U/R)$  and NEP (Figure 1-3). I am more curious about why some ecosystems (i.e. boreal ecosystems in Figure 2) seems to defy such correlation, and why the slope of this correlation (i.e. beta) changes spatially? Further discussions on these would be appreciated.*

Response: Thanks for this valuable suggestion.

For any year of each site, the indicator  $\beta$  was equivalent to the quotient between annual NEP and  $\ln(U/R)$ . Generally, the indicator  $\beta$  was convergent within-site and represents the site-level carbon uptake sensitivity. However, the indicator  $\beta$  would shift when an ecosystem experiences the serious disturbance, such as extreme heat waves and drought (Figure R1).

Therefore, the atmospheric inversion product presents low correlation between NEP and  $\ln(U/R)$  in some ecosystems because of the following two reasons: 1) the atmospheric inversion product was failed to capture the carbon uptake sensitivity in these boreal ecosystems; 2) these boreal ecosystems were experiencing serious disturbance that affect their carbon sink stability. In addition, the spatial variation in  $\beta$  reveals the differences of carbon uptake sensitivity across ecosystems.

We have added these discussions in the revised manuscript (Lines 296-303): “Thus, a sudden shift of the  $\beta$ -value may be an important early-warning signal for the critical transition of carbon uptake sensitivity of an ecosystem. In this study, the atmospheric inversion product shows low correlation between NEP and  $\ln(U/R)$  in some boreal ecosystems, which might due to that the atmospheric inversion product is failed to capture the carbon uptake sensitivity in these boreal ecosystems or these boreal ecosystems are experiencing serious disturbances. In addition, the spatial variation in  $\beta$  reveals the differences of carbon uptake sensitivity across ecosystems”.

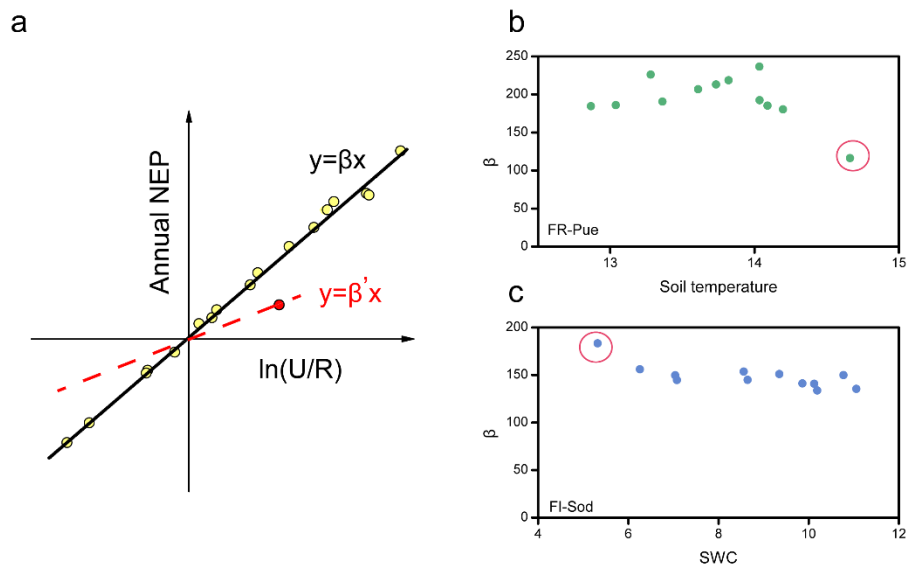


Figure R1. (a) The relationship between annual NEP and  $\ln(U/R)$  at a specific site. (b, c) Shift of indicator  $\beta$  in some specific sites along soil moisture and temperature.

Comment 2: For latter, the variation in beta is suggested to be related to  $I_{AV\_NEP}$ , which is regarded as an indicator of the carbon sink stability. Wouldn't  $I_{AV\_NEP}$  normalized by mean NEP make more sense here? I would be curious to see if there is a relationship between normalized  $I_{AV\_NEP}$  and beta, as sites with larger NEP seem more likely to have larger beta.

Response: Thanks for this suggestion.

First, the site-level mean annual NEP includes both negative and positive values, and therefore the  $I_{AV\_NEP}$  was quantified as the standard deviation of annual NEP rather than the normalized value. This approach have been widely used in the previous studies (Baldocchi et al., 2018; Marcolla et al., 2017).

Second, as suggested by the reviewer, we have tested the relationship between mean annual NEP and  $\beta$ , and found low correlation between mean annual NEP and  $\beta$  (Figure R2).

Third, the  $I_{AV\_NEP}$  in this study represents both the intensity and amplitude of variation in terrestrial carbon sink. Therefore, we prefer to use standard deviation of annual NEP to represent its inter-annual variation.

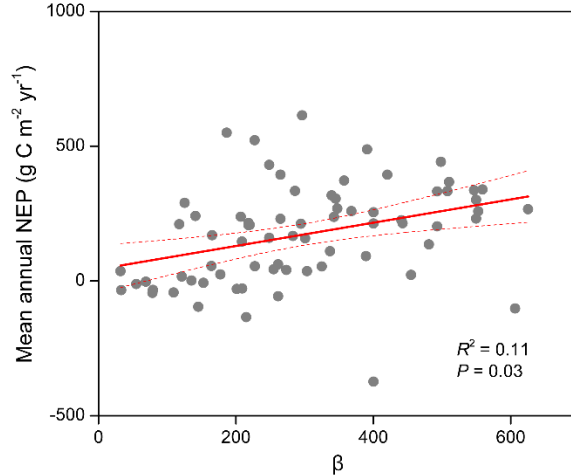


Figure R2. The relationship between mean annual NEP and the indicator  $\beta$ .

Marcolla, B., Rödenbeck, C., & Cescatti, A. (2017). Patterns and controls of inter-annual variability in the terrestrial carbon budget. *Biogeosciences*, 14(16), 3815-3829.

Baldocchi, D., Chu, H., & Reichstein, M. (2018). Inter-annual variability of net and gross ecosystem carbon fluxes: A review. *Agricultural and Forest Meteorology*, 249, 520-533.

Comment 3: *Figure 3a presents the correlation between annual mean NEP and  $\ln(U/R)$  across sites. I think there is a need to clarify the calculation of  $\ln(U/R)$  here as this indicator changes year-to-year for each site (did you use the mean  $\ln(U/R)$  of each site?).*

Response: Yes, Figure 3a shows the spatial correlation between annual mean NEP and mean  $\ln(U/R)$  of each site. We have added this information in Lines 204-205 as “Across the 72 flux-tower sites, the across-site variation in mean annual NEP were significantly correlated to mean annual  $\ln\left(\frac{U}{R}\right)$  of each site ( $R^2 = 0.65$ ,  $P < 0.01$ ) (Fig. 3a)”.

Comment 4: *It would be helpful to give more details on Equation (6). I could not understand how to decompose  $\ln(U/R)$  into the two components from what is presented here, but the method seems critical to Figure 4. Is equation (6) a multivariate linear function?*

Response: Thanks for this suggestion.

First, we have revised the expression of equation (6) as (Lines 161-167): “We further quantified the relative contributions of  $\frac{\bar{U}}{\bar{R}}$  and  $\frac{CUP}{CRP}$  in driving the spatial variations in NEP:

$$NEP = \beta \cdot \left[ \ln\left(\frac{\bar{U}}{\bar{R}}\right) + \ln\left(\frac{CUP}{CRP}\right) \right] \quad (5)$$

For a specific ecosystem, the parameter  $\beta$  was constant. Then, we used a relative importance analysis method to quantify the relative contributions of these two ratios to

the spatial variations in NEP”.

Second, the reviewer was right that we quantified the contributions of explanatory variables with a multiple linear regression model. The method was illustrated in Lines 186-189.



1 **Research article**

2 **Title**

3 Spatial variations in terrestrial net ecosystem productivity and its local indicators

4 **Running title**

5 Spatial variability in terrestrial NEP

6 **Authors**

7 Erqian Cui<sup>1,2</sup> (eqcui@stu.ecnu.edu.cn)

8 Chenyu Bian<sup>1,2</sup> (cybian@stu.ecnu.edu.cn)

9 Yiqi Luo<sup>3</sup> (yiqi.luo@nau.edu)

10 Shuli Niu<sup>4,5</sup> (sniu@igsnr.ac.cn)

11 Yingping Wang<sup>6</sup> (Yingping.Wang@csiro.au)

12 Jianyang Xia<sup>1,2,\*</sup> (jyxia@des.ecnu.edu.cn)

13 **Affiliations**

14 <sup>1</sup>Zhejiang Tiantong Forest Ecosystem National Observation and Research Station, Shanghai  
15 Key Lab for Urban Ecological Processes and Eco-Restoration, School of Ecological and  
16 Environmental Sciences, East China Normal University, Shanghai 200241, China;

17 <sup>2</sup>Research Center for Global Change and Ecological Forecasting, East China Normal University,  
18 Shanghai 200241, China;

19 <sup>3</sup>Center for ecosystem science and society, Northern Arizona University, Arizona, Flagstaff, AZ  
20 86011, USA.

21 <sup>4</sup>Key Laboratory of Ecosystem Network Observation and Modeling, Institute of Geographic  
22 Sciences and Natural Resources Research, Chinese Academy of Sciences, Beijing, China;

23 <sup>5</sup>University of Chinese Academy of Sciences, Beijing, China;

24 <sup>6</sup>CSIRO Oceans and Atmosphere, PMB 1, Aspendale, Victoria 3195, Australia.

25 **Correspondence**

26 Jianyang Xia, School of Ecological and Environmental Sciences, East China Normal University,  
27 Shanghai 200241, China.

28 Email: jyxia@des.ecnu.edu.cn

29 **Key words**

30 Net ecosystem productivity, spatial variation, net CO<sub>2</sub> uptake and release, local indicators,  
31 model

32 **Abstract**

33 Multiple lines of evidence have demonstrated the persistence of global land carbon (C) sink  
34 during the past several decades. However, both annual net ecosystem productivity (NEP) and  
35 its inter-annual variation ( $I_{AV_{NEP}}$ ) keep varying over space. Thus, identifying local indicators  
36 for the spatially varying NEP and  $I_{AV_{NEP}}$  is critical for locating the major and sustainable C  
37 sinks on the land. Here, based on daily NEP observations from FLUXNET sites and large-scale  
38 estimates from anthe atmospheric inversion product, we found a robust logarithmic correlation  
39 between annual NEP and seasonal carbon uptake-release ratio of total CO<sub>2</sub> exchanges  
40 during net uptake (U) and release (R) periods (i.e.,  $U/R$ ). The cross-site variation of mean annual  
41 NEP could be logarithmically linearly indicated by  $\ln(U/R)$ , while the spatial distribution of  
42  $I_{AV_{NEP}}$  was well indicated by associated with the slope (i.e.,  $\beta$ ) of the ~~demonstrated~~ logarithmic  
43 correlation between annual NEP and  $U/R$ . Among biomes, for example, forests and croplands  
44 had the largest  $U/R$  ratio ( $1.06 \pm 0.83$ ) and  $\beta$  ( $473 \pm 112 \text{ g C m}^{-2} \text{ yr}^{-1}$ ), indicating the highest NEP  
45 and  $I_{AV_{NEP}}$  in forests and croplands, respectively. We further showed that these two simple  
46 indicators could directly infer the spatial variations ~~in~~ of NEP and  $I_{AV_{NEP}}$  in global gridded NEP  
47 products. Overall, this study provides two simple local indicators for the intricate spatial  
48 variations in the strength and stability of land C sinks. These indicators could be helpful for  
49 locating the persistent terrestrial C sinks and provides valuable constraints for improving the  
50 simulation of land-atmospheric C exchanges.

51

## 52 1. Introduction

53 Terrestrial ecosystems reabsorb about one-quarter of anthropogenic CO<sub>2</sub> emission (Ciais et  
54 al., 2019) and are primarily responsible for the recent temporal fluctuations of the measured  
55 atmospheric CO<sub>2</sub> growth rate (Randerson, 2013; Le Quéré et al., 2018). In addition, evidence  
56 based on eddy-flux measurements (Baldocchi et al., 2018; Rödenbeck et al., 2018), aircraft  
57 atmospheric budgets (Peylin et al., 2013), and process-based model simulations (Poulter et al.,  
58 2014; Ahlstrom et al., 2015) has shown a large spatial variability in net ecosystem productivity  
59 (NEP) on the land. The elusive variation of terrestrial NEP over space refers to both of the  
60 substantial varying mean annual NEP and the divergent inter-annual variability (IAV) in NEP  
61 (i.e., IAV<sub>NEP</sub>; usually quantified as the standard deviation of annual NEP) across space  
62 (Baldocchi et al., 2018; Marcolla et al., 2017). The mean annual NEP is related to the strength  
63 of carbon exchange of a specific ecosystem (Randerson et al., 2002; Luo and Weng, 2011; Jung  
64 et al., 2017), while IAV<sub>NEP</sub> characterizes the stability of such carbon exchange (Musavi et al.,  
65 2017). Thus, whether and how NEP and IAV<sub>NEP</sub> change over the space is important for  
66 predicting the future locations of carbon sinks on the land (Yu et al., 2014; Niu et al., 2017).

67 Large spatial difference in terrestrial NEP has been reported from eddy-flux measurements,  
68 model outputs and atmospheric inversion products. In addition, the global average IAV of NEP  
69 was large relative to global annual mean NEP (Baldocchi et al., 2018). More importantly, the  
70 spatial variations of NEP and IAV<sub>NEP</sub> were typically underestimated by the global flux tower-  
71 based product~~compiled global product~~ and the process-based global models (Jung et al., 2020;  
72 Fu et al., 2019). These discrepancies further revealed the necessary to identify local indicators  
73 for the spatially varying NEP and IAV<sub>NEP</sub>, separately. The NEP in terrestrial ecosystems is  
74 determined by two components, including vegetation photosynthesis and ecosystem respiration  
75 (Reichstein et al., 2005), ~~and their relative difference~~ Because photosynthesis and respiration  
76 are strongly correlated over space ~~(Baldocchi et al., 2015; Biederman et al., 2016), their relative~~  
77 difference ~~could determine the spatial variation of NEP~~ (Baldocchi et al., 2015; Biederman et  
78 al., 2016). Many previous analyses have attributed the IAV<sub>NEP</sub> at the site level to the different  
79 sensitivities of ecosystem photosynthesis and respiration to environmental drivers (Gilmanov et  
80 al., 2005; Reichstein et al., 2005) and biotic controls (Besnard et al., 2018; Musavi et al., 2017).

81 For example, some studies have reported that  $IAV_{NEP}$  is more associated with variations in  
82 photosynthesis than carbon release (Ahlstrom et al., 2015; Novick et al., 2015; Li et al., 2017),  
83 whereas others have indicated that respiration is more sensitive to anomalous climate variability  
84 (Valentini et al., 2000; von Buttlar et al., 2017). However, despite the previous efforts in a  
85 predictive understanding of the land-atmospheric C exchanges, the multi-model spread has not  
86 reduced over time (Arora et al., 2019). Therefore, it is imperative to explore the potential  
87 indicators for the spatially varying NEP, which could help attribute the spatial variation of NEP  
88 and  $IAV_{NEP}$  into different processes and provide valuable constraints for the global C cycle.  
89 Alternatively, the annual NEP of a given ecosystem can be also directly decomposed into net  
90  $CO_2$  uptake flux and  $CO_2$  release flux (Gray et al., 2014), which are more direct components for  
91 NEP (Fu et al., 2019). ~~Many studies have reported that the vegetation  $CO_2$  uptake during the~~  
92 ~~growing season and the non-growing season soil respiration are tightly correlated (Luo et al.,~~  
93 ~~2014; Zhao et al., 2016).~~ It is still unclear how the ecosystem net  $CO_2$  uptake and release fluxes  
94 would control the spatially varying NEP.

95 Conceptually, the total net  $CO_2$  uptake flux ( $U$ ) is determined by the length of  $CO_2$  uptake  
96 period ( $CUP$ ) and the  $CO_2$  uptake rate, while the total net  $CO_2$  release flux ( $R$ ) depends on the  
97 length of  $CO_2$  release period ( $CRP$ ) and the  $CO_2$  release rate (Fig. 1b). The variations of NEP  
98 thus ~~should~~ could be ~~innovatively~~ attributed to these decomposed components. A strong spatial  
99 correlation between mean annual NEP and length of  $CO_2$  uptake period has been reported in  
100 evergreen needle- and broad-leaved forests (Churkina et al., 2005; Richardson et al., 2013;  
101 Keenan et al., 2014), whereas atmospheric inversion data and vegetation photosynthesis model  
102 indicated a dominant role of the maximal carbon uptake rate (Fu et al., 2017; Zhou et al., 2017).  
103 However, the relative importance of these phenological and physiological indicators for the  
104 spatially varying NEP remains unclear.

105 In this study, we decomposed annual NEP into  $U$  and  $R$ , and explored the local indicators  
106 for spatially varying NEP. Based on the eddy-covariance fluxes from FLUXNET2015 Dataset  
107 (Pastorello et al., 2017) and the atmospheric inversion product (Rödenbeck et al., 2018), we  
108 examined the relationship between NEP and its direct components. In addition, we used the  
109 observations to evaluate the spatial variations of NEP and  $IAV_{NEP}$  in the FLUXCOM product

110 and a process-based model (CLM4.5) (Oleson et al., 2013). The major aim of this study is to  
111 explore whether there are useful local indicators for the spatially varying NEP and IAV<sub>NEP</sub> in  
112 terrestrial ecosystems.

## 113 **2. Materials and Methods**

### 114 **2.1 Datasets**

115 Daily NEP observations of eddy covariance sites are obtained from the FLUXNET2015 Tier 1  
116 dataset (<http://fluxnet.fluxdata.org/data/fluxnet2015-dataset/>). The FLUXNET2015 dataset  
117 provides half-hourly data of carbon, water and energy fluxes at over 210 sites that are  
118 standardized and gap-filled (Pastorello et al., 2017). However, time series of most sites are still  
119 too short for the analysis of inter-annual variation in NEP. So only the sites that provided the  
120 availability of eddy covariance flux measurements for at least 5 years are selected. This leads to  
121 a global dataset of 72 sites with different biomes across different climatic regions. Based on the  
122 biome classification from the International Geosphere-Biosphere Programme (IGBP) provided  
123 for the FLUXNET2015 sites, the selected sites include 35 forests (FOR), 15 grasslands (GRA),  
124 11 croplands (CRO), 4 wetlands (WET), 2 shrublands (SHR) and 5 savannas (SAV) (Fig. S1  
125 and Table S1).

126 The Jena CarboScope Inversion product compiles from high precision measurements of  
127 atmospheric CO<sub>2</sub> concentration with simulated atmospheric transport to infer the net CO<sub>2</sub>  
128 exchanges between land, ocean and atmosphere at large scales (Rödenbeck et al., 2018). Here,  
129 we used the daily land-atmosphere CO<sub>2</sub> fluxes from the s85\_v4.1 version at a spatial resolution  
130 of 5° × 3.75°. Considering the relatively low spatial resolution of the Jena Inversion product, the  
131 daily fluxes were only used to calculate the local indicators for the spatially varying NEP at the  
132 global scale.

133 Daily NEP simulations from Community Land Model version 4.5 (CLM4.5) were also used  
134 to calculate the local indicators for the spatially varying NEP at the corresponding flux tower  
135 sites. We ran the CLM4.5 model from 1985 to 2010 at a spatial resolution of 1° with CRUNECIP  
136 meteorological forcing. Here, NEP was derived as the difference between GPP and TER, and  
137 TER was calculated as the sum of simulated autotrophic and heterotrophic respiration. The daily

138 outputs from CLM4.5 were used to calculate the local indicators for the spatially varying NEP  
139 both at the global scale and at the FLUXNET site level.

140 The FLUXCOM product presents an upscaling of carbon flux estimates from 224 flux  
141 tower sites based on multiple machine learning algorithms and meteorological drivers (Jung et  
142 al., 2017). To be consistent with the meteorological forcing of Jena Inversion product and the  
143 CLM4.5 model, we used the FLUXCOM CRUNCEPv6 products. In addition, in order to reduce  
144 the uncertainty caused by machine-learning methods, we averaged all the FLUXCOM  
145 CRUNCEPv6 products with different machine-learning methods. It should be noted that the  
146 inter-annual variability of FLUXCOM product is ~~only~~ driven by ~~climatic~~  
147 ~~conditions~~ meteorological measurements and satellite data, which partially includes information  
148 on vegetation state and other land surface properties ~~the effects of land use and land cover change~~  
149 ~~are not represented~~. The FLUXCOM NEP product is downloaded from the Data Portal of the  
150 Max Planck Institute for Biochemistry ([https://www.bgc-](https://www.bgc-jena.mpg.de/geodb/projects/Home.php)  
151 [jena.mpg.de/geodb/projects/Home.php](https://www.bgc-jena.mpg.de)~~https://www.bgc-jena.mpg.de~~). Daily outputs from  
152 FLUXCOM for the period 1985-2010 at 0.5° spatial resolution were used to calculate the local  
153 indicators for the spatially varying NEP both at the global scale and at the FLUXNET site level.

## 154 2.2 Decomposition of NEP and the calculations for its local indicators

155 The annual NEP of a given ecosystem can be defined numerically as the difference between the  
156 net CO<sub>2</sub> uptake and release ~~(Figure 2b). These. As illustrated in Figure 2b:~~

$$157 \text{-----} \text{NEP} = U - R \text{-----} (1)$$

158 ~~These~~ components of NEP contain both photosynthesis and respiration flux, which directly  
159 indicate the net CO<sub>2</sub> exchange of an ecosystem. The total net CO<sub>2</sub> uptake flux ( $U$ ) and the total  
160 net CO<sub>2</sub> release flux ( $R$ ) can be further decomposed as:

$$161 U = \bar{U} \times CUP$$
$$162 (21)$$

$$R = \bar{R} \times CRP$$

(32)

where  $CUP$  ( $d yr^{-1}$ ) is the length of  $CO_2$  uptake period and  $CRP$  ( $d yr^{-1}$ ) is the length of  $CO_2$  release period; the  $\bar{U}$  ( $g C m^{-2} d^{-1}$ ) is the mean daily net  $CO_2$  uptake over  $CUP$  ( $d yr^{-1}$ ) and  $\bar{R}$  ( $g C m^{-2} d^{-1}$ ) represents the mean daily net  $CO_2$  release over  $CRP$  ( $d yr^{-1}$ ). Many studies have reported that the vegetation net  $CO_2$  uptake during the growing season and the non-growing season soil net  $CO_2$  release are tightly correlated (Luo et al., 2014; Zhao et al., 2016). ~~In addition~~ Therefore, we further tested the relationship between annual NEP and ~~the ratio of~~  $\frac{U}{R}$  (i.e.,  $NEP \propto \frac{U}{R}$ ), which reflects. ~~Ecologically, the ratio of~~  $\frac{U}{R}$  reflects the seasonal carbon uptake-release ratio ~~relative strength of the ecosystem  $CO_2$  uptake.~~ Therefore ~~Consequently~~, NEP in ~~any year of~~ any given ecosystem can be expressed as (Fig. S2):

$$NEP = \beta \cdot \ln\left(\frac{U}{R}\right) \quad (43)$$

where the parameter  $\beta$  represents the slope of the linear relationship of  $NEP \propto \ln\left(\frac{U}{R}\right)$ , indicating the site-level carbon uptake sensitivity. Based on the definitions of  $U$  and  $R$ , the ratio  $\frac{U}{R}$  can be further written as:

$$\frac{U}{R} = \frac{\bar{U}}{\bar{R}} \cdot \frac{CUP}{CRP} \quad (54)$$

Ecologically, the ratio of  $\frac{\bar{U}}{\bar{R}}$  reflects the relative physiological difference between ecosystem  $CO_2$  uptake and release strength, while the ratio of  $\frac{CUP}{CRP}$  is an indicator of net ecosystem  $CO_2$  exchange phenology. Environmental changes may regulate these ecological processes and ultimately affect the ecosystem NEP. The slope  $\beta$  indicates the response sensitivity of NEP to the changes in phenology and physiological processes. All of  $\beta$ ,  $\frac{CUP}{CRP}$  and  $\frac{\bar{U}}{\bar{R}}$  were then calculated from the selected eddy covariance sites and the corresponding pixels of these sites in models. These derived indicators from eddy covariance sites were then used to benchmark the results extracted from the same locations in models.

## 2.4 Calculation of the relative contributions

188 We further quantified the relative contributions of  $\frac{\bar{U}}{\bar{R}}$  and  $\frac{CUP}{CRP}$  in driving the spatial variations  
189 in NEP:

$$190 \quad \text{NEP} = \beta \cdot \left[ \ln \left( \frac{\bar{U}}{\bar{R}} \right) + \ln \left( \frac{CUP}{CRP} \right) \right] f \left( \frac{\bar{U}}{\bar{R}}, \frac{CUP}{CRP} \right) \quad \text{---}$$

191 (65)

192 For a specific ecosystem, the parameter  $\beta$  was constant. Then, We-we used a relative  
193 importance analysis method to quantify the relative contributions of each-these two ratios to the  
194 spatial variations in NEP. The algorithm was performed with the “ralaimpo” package in R (R  
195 Development Core Team, 2011). The “relaimpo” package is based on variance decomposition  
196 for multiple linear regression models. We chose the most commonly used method named  
197 “Lindeman-Merenda-Gold (LMG)” (Grömping, 2007) from the methods provided by the  
198 “ralaimpo” package. This method allows us to quantify the contributions of explanatory  
199 variables in a multiple linear regression model. Across the 72 FLUXNET sites, we quantified  
200 the relative importance of  $\frac{\bar{U}}{\bar{R}}$  and  $\frac{CUP}{CRP}$  to cross-site changes in NEP.

### 201 3. Results

#### 202 3.1 The relationship between NEP and its direct components

203 To find local indicators for the spatially varying NEP in terrestrial ecosystems, we tested the  
204 relationship between NEP and its direct components ( $U$  and  $R$ ) across the 72 flux-tower sites.  
205 The results showed that annual NEP was closely related with the ratio of  $\frac{U}{R}$  (Fig. S2). The  
206 logarithmic correlations between annual NEP and  $\frac{U}{R}$  were significant at all sites (Fig. 1a), and  
207 ~90% of  $R^2$  falling within a range from 0.7 to 1 (Fig. 1c).

208 In addition, the relationship between NEP and  $\frac{U}{R}$  was also ~~verified~~confirmed by the  
209 atmospheric inversion product (i.e., Jena CarboScope Inversion). The control of  $\frac{U}{R}$  on annual  
210 NEP was robust in most global grid cells (i.e.  $0.6 < R^2 < 1$ ). The explanation of  $\frac{U}{R}$  was higher  
211 in 80% of the regions, but lower in North American (Fig. 2). These two datasets both showed  
212 that the indicator  $\frac{U}{R}$  could successfully capture the variability in annual NEP.



### 213 3.2 Local indicators for spatially varying NEP

214 Across the 72 flux-tower sites, the ~~across-site variations~~ ~~spatial changes~~ in mean annual NEP were  
215 significantly correlated to ~~mean annual~~  $\ln\left(\frac{U}{R}\right)$  ~~of each site~~ ( $R^2 = 0.65, P < 0.01$ ) (Fig. 3a). This  
216 finding suggested that the mean annual ratio  $\ln\left(\frac{U}{R}\right)$  is a good indicator for cross-site variation  
217 in NEP. By contrast, the spatial variation of  $\text{IAV}_{\text{NEP}}$  was moderately explained by the slope (i.e.,  
218  $\beta$ ) of the temporal correlation between NEP and  $\ln\left(\frac{U}{R}\right)$  at each site ( $R^2 = 0.39, P < 0.01$ ; Fig.  
219 3b) rather than  $\ln\left(\frac{U}{R}\right)$  (Fig. S3). The wide range of ratio  $\beta$  reveals a large divergence of NEP  
220 sensitivity across biomes, ranging from  $121 \pm 118 \text{ g C m}^{-2} \text{ yr}^{-1}$  in shrubland to  $473 \pm 112 \text{ g C m}^{-2}$   
221  $\text{yr}^{-1}$  in cropland.

222 The decomposition of indicator  $\frac{U}{R}$  into  $\frac{\bar{U}}{\bar{R}}$  and  $\frac{CUP}{CRP}$  allowed us to quantify the relative  
223 importance of these two ratios in driving NEP variability. The linear regression and relative  
224 importance analysis showed a more important role of  $\frac{CUP}{CRP}$  (58%) than  $\frac{\bar{U}}{\bar{R}}$  (42%) in explaining  
225 the cross-site variation of NEP (Fig. 4). Therefore, the spatial distribution of mean annual NEP  
226 was ~~more strongly~~ ~~mostly~~ driven by the phenological ~~rather than physiological~~ changes.

### 227 3.3 Simulated spatial variations in NEP by models

228 We further used these two simple indicators (i.e.,  $\frac{U}{R}$  and  $\beta$ ) to evaluate the simulated spatial  
229 variations of NEP by the ~~global flux tower-based~~ ~~compiled~~ ~~global~~ product (i.e., FLUXCOM)  
230 and a widely-used process-based model at the FLUXNET site level (i.e., CLM4.5). We found  
231 that the low spatial variation of mean annual NEP in FLUXCOM and CLM4.5 could be inferred  
232 from their more converging  $\ln\left(\frac{U}{R}\right)$  than flux-tower measurements (Fig. 5). The underestimated  
233 variation of  $\text{IAV}_{\text{NEP}}$  in these modeling results was also clearly shown by the smaller  $\beta$  values  
234 (268.22, 126.00 and 145.08 for FLUXNET, FLUXCOM and CLM4.5, respectively) (Fig. 5b).

235 In addition, the spatial variations of NEP and  $\text{IAV}_{\text{NEP}}$  were associated with the spatial  
236 resolution of the product (Marcolla et al., 2017). Considering the scale mismatch between  
237 FLUXNET sites and the gridded product, we run the same analysis at the global scale based on  
238 Jena Inversion product. At the global scale, the spatial variation of mean annual NEP can be also

239 well indicated by  $\ln\left(\frac{U}{R}\right)$  (Fig. 6). The larger net C uptake in FLUXCOM resulted from its  
240 higher simulations for  $\ln\left(\frac{U}{R}\right)$ . Furthermore, the larger spatial variation of  $I_{AV_{NEP}}$  in CLM4.5  
241 could be inferred from the indicator  $\beta$ .

## 242 4. Discussion

### 243 4.1 New perspective for locating the major and sustainable land C sinks

244 Large spatial differences of mean annual NEP and  $I_{AV_{NEP}}$  have been well-documented in  
245 previous studies (Jung et al., 2017; Marcolla et al., 2017; Fu et al., 2019). Here we provide a  
246 new perspective for quantifying the spatially varying NEP by tracing annual NEP into several  
247 local indicators. Therefore, these traceable indicators could provide useful constraints for  
248 predicting annual NEP, especially in areas without eddy-covariance towers.

249 Typically, the C sink capacity and its stability of a specific ecosystem are characterized  
250 separately (Keenan et al., 2014; Ahlstrom et al., 2015; Jung et al., 2017). Here we integrated  
251 NEP into two simple indicators that could directly locate the major and sustainable land C sink.  
252 Among biomes, forests and croplands had the largest  $\ln\left(\frac{U}{R}\right)$  and  $\beta$ , indicating the strongest and  
253 the most unstable C sink in forests and croplands, respectively. However, the relatively lower  $\beta$   
254 in shrublands and savannas should be interpreted cautiously. There are very few semi-arid  
255 ecosystems in the FLUXNET sites, while they represent a large portion of land at the global  
256 scale and have been shown to substantially control the interannual variability of NEP (Ahlström  
257 et al., 2015). The highest  $\beta$  ~~in croplands implies that the land covered by cropland with the~~  
258 ~~largest  $I_{AV_{NEP}}$ . Therefore, implies that the reported~~ rapid global expansion of cropland may  
259 enlarge the ~~fluctuations in Land-atmosphere  $CO_2$  exchange  $I_{AV_{NEP}}$  on the land.~~ In fact, the  
260 cropland expansion has been confirmed as one important driver of the recent increasing global  
261 vegetation growth peak (Huang et al., 2018) and atmospheric  $CO_2$  seasonal amplitude (Gary et  
262 al., 2014; Zeng et al., 2014).

### 263 4.2 Joint control of plant phenology and physiology on mean annual NEP 264 dominant spatial distribution of mean annual NEP

265 Recent studies have demonstrated that the spatiotemporal variations in terrestrial gross primary

266 productivity are jointly controlled by plant phenology and physiology (Xia et al., 2015; Zhou et  
267 al., 2016). Here we demonstrated ~~that the spatial difference of mean annual NEP the dominant~~  
268 ~~role of~~ ~~was determined by both~~ the phenology indicator  $\frac{CUP}{CRP}$  (58%) ~~in driving and the~~  
269 ~~physiological indicator~~  $\frac{\bar{U}}{\bar{R}}$  (42%) ~~the spatial difference of mean annual NEP. In addition, The~~  
270 ~~the reported low lower correlation between mean annual NEP and contribution of the~~  
271 ~~physiological indicator~~ ~~or could~~ ~~or~~  $\frac{\bar{U}}{\bar{R}}$  ~~could~~ partly be attributed to the convergence of  $\frac{\bar{U}}{\bar{R}}$  across  
272 FLUXNET sites (Fig. S4).

273 The convergent  $\frac{\bar{U}}{\bar{R}}$  across sites was first discovered by Churkina *et al.* (2005) as  $2.73 \pm 1.08$   
274 across 28 sites, which included DBF, EBF and crop/grass. In this study, we found the  $\frac{\bar{U}}{\bar{R}}$  across  
275 the 72 sites is  $2.71 \pm 1.61$ , which validates the discovery by Churkina *et al.* However, the  $\frac{\bar{U}}{\bar{R}}$   
276 varied among biomes ( $2.86 \pm 1.56$  for forest,  $2.16 \pm 1.14$  for grassland,  $3.47 \pm 1.98$  for cropland,  
277  $2.89 \pm 1.47$  for wetland,  $1.89 \pm 1.10$  for shrub,  $1.83 \pm 0.88$  for savanna). This spatial convergence  
278 of  $\frac{\bar{U}}{\bar{R}}$  at the ecosystem level provides important constraints for global models that simulate  
279 various physiological processes (Peng et al., 2015; Xia et al., 2017). These findings imply that  
280 the phenology changes will greatly affect the locations of the terrestrial carbon sink by  
281 modifying the length of carbon uptake period (Richardson et al., 2013; Keenan et al., 2014).

#### 282 4.3 The simulated local indicators from gridded products

283 This study showed that the considerable spatial variations in mean annual NEP and  $IAV_{NEP}$  from  
284 global gridded products could also be inferred from their local indicators. The low variations of  
285  $\frac{U}{R}$  ratio in CLM4.5 could be largely due to their simple representations of the diverse terrestrial  
286 plant communities into a few plant functional types with parameterized properties (Cui et al.,  
287 2019; Sakschewski et al., 2015). In addition, the higher  $\frac{U}{R}$  ratio from FLUXCOM product  
288 indicated its widely reported larger net C uptake (Fig. 6) (Jung et al., 2020). Meanwhile, the  
289 ignorance of fire, land-use change and other disturbances could lead to the smaller  $\beta$  by allowing  
290 for only limited variations of phenological and physiological dynamics (Reichstein et al., 2014;  
291 Kunstler et al., 2016). Although the magnitude of  $IAV_{NEP}$  depends on the spatial resolution

292 (Marcolla et al., 2017), we recommend future model benchmarking analyses to use not only the  
293 global product compiled from machine-learning method (Bonan et al., 2018) but also the site-  
294 level measurements or indicators (Xia et al., 2020i.e.,  $\ln\left(\frac{U}{R}\right)$  and  $\beta$ ).

#### 295 **4.4 Conclusions and further implications**

296 In summary, this study highlights the changes in NEP and  $IAV_{NEP}$  over space on the land, and  
297 provides the  $\frac{U}{R}$  ratio and  $\beta$  as two simple local indicators for their spatial variations. These  
298 indicators could be helpful for locating the persistent terrestrial C sinks in where the  $\ln\left(\frac{U}{R}\right)$   
299 ratio is high but the  $\beta$  is low. Their estimates based on observations are also valuable for  
300 benchmarking and improving the simulation of land-atmospheric C exchanges in Earth system  
301 models.

302 ~~In addition,~~ The findings in this study have some important implications for understanding the  
303 variation of NEP on the land. First, forest ecosystems have the largest annual NEP due to the  
304 largest  $\ln\left(\frac{U}{R}\right)$  while croplands show the highest  $IAV_{NEP}$  because of the highest  $\beta$ . Second, the  
305 spatial convergence of  $\frac{\bar{U}}{\bar{R}}$  suggests a tight linkage between plant growth and the non-growing  
306 season soil microbial activities (Xia et al., 2014; Zhao et al., 2016). However, it remains unclear  
307 whether the inter-biome variation in  $\frac{\bar{U}}{\bar{R}}$  is due to different plant-microbe interactions between  
308 biomes.— ~~Third~~ Third, the within-site convergent but spatially varying  $\beta$  needs better  
309 understanding. Previous studies have shown that a rising standard deviation of ecosystem  
310 functions could indicate an impending ecological state transition (Carpenter and Brock, 2006;  
311 Scheffer et al., 2009). Thus, a sudden shift of the  $\beta$ -value may be an important early-warning  
312 signal for the critical transition of ~~carbon uptake sensitivity of  $IAV_{NEP}$  of~~ an ecosystem. In this  
313 study, the atmospheric inversion product shows low correlation between NEP and  $\ln\left(\frac{U}{R}\right)$  in  
314 some boreal ecosystems, which might due to that the atmospheric inversion product is failed to  
315 capture the carbon uptake sensitivity in these boreal ecosystems or these boreal ecosystems are  
316 experiencing serious disturbances. Therefore, the robustness in relationship between annual  
317 NEP and  $\ln\left(\frac{U}{R}\right)$  depends on the temporal stability of carbon uptake sensitivity for an ecosystem.

318 In addition, the spatial variation in  $\beta$  reveals the differences of carbon uptake sensitivity across  
319 ecosystems. Furthermore, considering the limited eddy-covariance sites with long-term  
320 observations, these findings need further validation once the longer time-series of measurements  
321 from more sites and vegetation types become available.

## 322 **Acknowledgements**

323 This work was financially supported by the National Key R&D Program of China  
324 (2017YFA0604600), National Natural Science Foundation of China (31722009, 41630528) and  
325 National 1000 Young Talents Program of China. This work used eddy covariance dataset  
326 acquired and shared by the FLUXNET community, including these networks: AmeriFlux,  
327 AfriFlux, AsiaFlux, CarboAfrica, CarboEuropeIP, CarboItaly, CarboMont, ChinaFlux, Fluxnet-  
328 Canada, GreenGrass, ICOS, KoFlux, LBA, NECC, OzFlux-TERN, TCOS-Siberia, and USCCC.  
329 The ERA-Interim reanalysis data are provided by ECMWF and processed by LSCE. The  
330 FLUXNET eddy covariance data processing and harmonization was carried out by the European  
331 Fluxes Database Cluster, AmeriFlux Management Project, and Fluxdata project of FLUXNET,  
332 with the support of CDIAC and ICOS Ecosystem Thematic Center, and the OzFlux, ChinaFlux  
333 and AsiaFlux offices.

334 *Data availability statement.* Eddy flux data are available at  
335 <http://fluxnet.fluxdata.org/data/fluxnet2015-dataset/>; the data supporting the findings of this  
336 study are available within the article and the Supplementary Information.

337 *Author contribution.* E. Cui and J. Xia devised and conducted the analysis. Y. Luo, S. Niu, Y.  
338 Wang and C. Bian provided critical feedback on the method and results. All authors contributed  
339 to discussion of results and writing the paper.

340 *Competing interests.* The authors declare that there is no conflict of interest.

341 **FIGURES**

342 **Figure 1** Relationship between annual NEP and  $\frac{U}{R}$  for 72 FLUXNET sites (of the form  $NEP =$   
343  $\beta \cdot \ln\left(\frac{U}{R}\right)$ ). a, Dependence of annual NEP on the ratio between total CO<sub>2</sub> exchanges during net  
344 uptake ( $U$ ) and release ( $R$ ) periods (i.e.,  $\frac{U}{R}$ ). Each line represents one flux site with at least 5  
345 years of observations. b, Conceptual figure for the decomposition framework introduced in this  
346 study. Annual NEP can be quantitatively decomposed into the following indicators:  $NEP =$   
347  $U - R$ . c, Distribution of the explanation of  $\frac{U}{R}$  on temporal variability of NEP ( $R^2$ ) for  
348 FLUXNET sites.

349 **Figure 2** Relationship between annual NEP and  $\frac{U}{R}$  for Jena Inversion product (of the form  
350  $NEP = \beta \cdot \ln\left(\frac{U}{R}\right)$ ). The black box indicates the location of the sample.

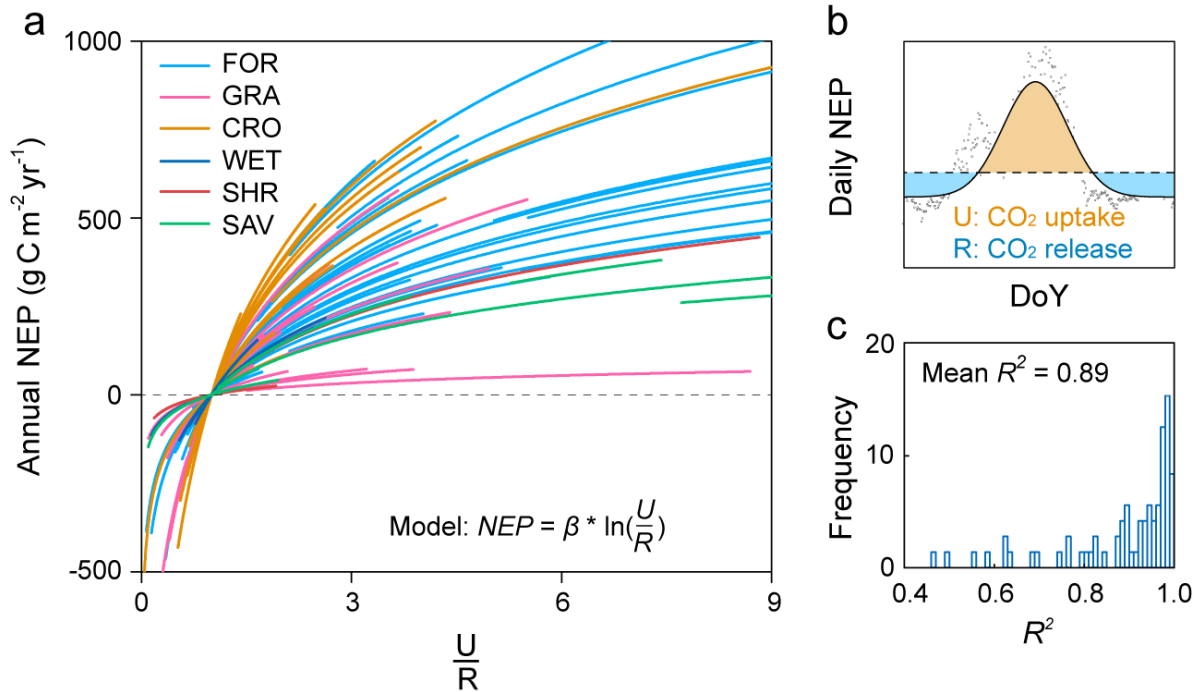
351 **Figure 3** Contributions of the two indicators in explaining the spatial patterns of mean annual  
352 NEP and  $IAV_{NEP}$ . a, The relationship between annual mean NEP and  $\ln\left(\frac{U}{R}\right)$  across FLUXNET  
353 sites ( $R^2 = 0.65, P < 0.01$ ). The insets show the variation of  $\ln\left(\frac{U}{R}\right)$  for different terrestrial  
354 biomes. b, The explanation of  $\beta$  on  $IAV_{NEP}$  ( $R^2 = 0.39, P < 0.01$ ). The insets show the distribution  
355 of parameter  $\beta$  for different terrestrial biomes. The number of site-years at each site is indicated  
356 with the size of the point.

357 **Figure 4** The linear regression between  $\frac{U}{R}$  with  $\frac{CUP}{CRP}$  ( $R^2 = 0.71, P < 0.01$ ) and  $\frac{\bar{U}}{\bar{R}}$  ( $R^2 = 0.09,$   
358  $P < 0.01$ ) across sites. The insets show the relative contributions of each indicator to the spatial  
359 variation of  $\frac{U}{R}$ . The number of site-years at each site is indicated with the size of the point.

360 **Figure 5** Representations of the spatially varying NEP and its local indicators in FLUXCOM  
361 product and the Community Land Model (CLM4.5) at the FLUXNET site level. a, The variation  
362 of mean annual NEP and  $IAV_{NEP}$  derives from FLUXNET, FLUXCOM and CLM4.5. Variation  
363 in mean annual NEP: the standard deviation of mean annual NEP across sites; Variation in  
364  $IAV_{NEP}$ : the standard deviation of  $IAV_{NEP}$  across sites. b, Representations of the local indicators  
365 for NEP in FLUXNET, FLUXCOM and CLM4.5. The corresponding distributions of  $\ln\left(\frac{U}{R}\right)$   
366 and  $\beta$  are shown at the top and right. Significance of the relationship between annual NEP and

367  $\ln\left(\frac{U}{R}\right)$  for each site is indicated by the circle: closed circles:  $P < 0.05$ ; open circles:  $P > 0.05$ . Note  
368 that the modeled results are from the pixels extracted from the same locations of the flux tower  
369 sites.

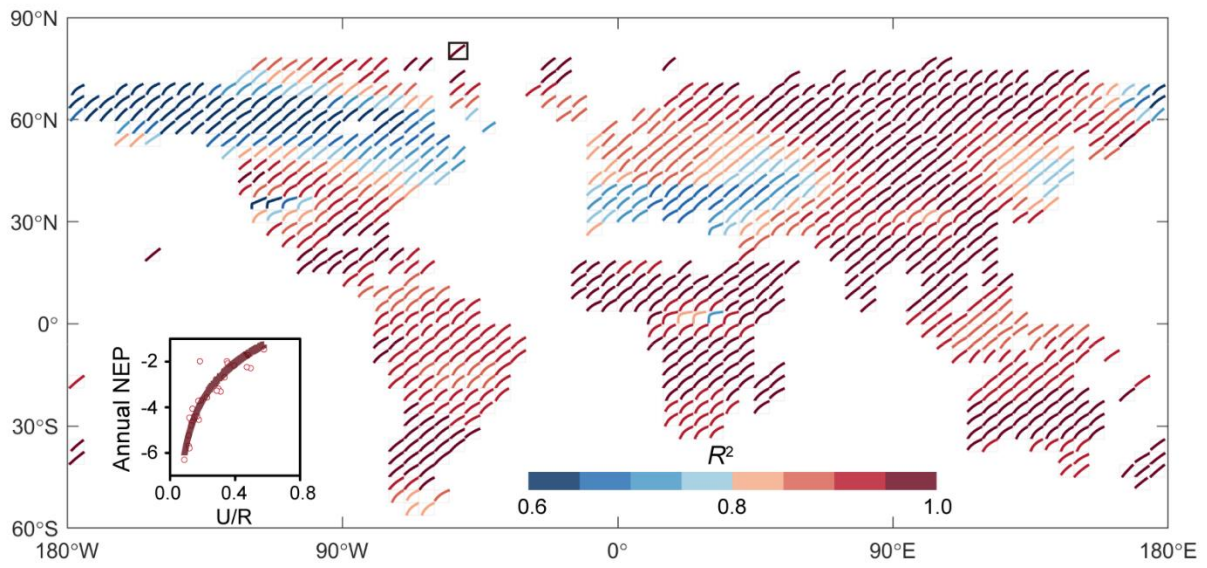
370 **Figure 6** Representations of the spatially varying NEP and its local indicators in FLUXCOM  
371 product and the Community Land Model (CLM4.5) at the global scale. a, The variation of mean  
372 annual NEP and  $I_{AV_{NEP}}$  derives from Jena Inversion, FLUXCOM and CLM4.5. Variation in  
373 mean annual NEP: the spatial variation of mean annual NEP; Variation in  $I_{AV_{NEP}}$ : the spatial  
374 variation of standard deviation in  $I_{AV_{NEP}}$ . b, Representations of the local indicators for NEP in  
375 Jena Inversion, FLUXCOM and CLM4.5.  
376



377  
 378 **Figure 1** Relationship between annual NEP and  $\frac{U}{R}$  for 72 FLUXNET sites (of the form  $NEP =$   
 379  $\beta \cdot \ln\left(\frac{U}{R}\right)$ ). **a**, Dependence of annual NEP on the ratio between total CO<sub>2</sub> exchanges during net  
 380 uptake ( $U$ ) and release ( $R$ ) periods (i.e.,  $\frac{U}{R}$ ). Each line represents one flux site with at least 5  
 381 years of data. **b**, Conceptual figure for the decomposition framework introduced in this study.  
 382 Annual NEP can be quantitatively decomposed into the following indicators:  $NEP = U - R$ . **c**,  
 383 Distribution of the explanation of  $\frac{U}{R}$  on temporal variability of FLUXNET NEP ( $R^2$ ) for  
 384 FLUXNET sites.

385



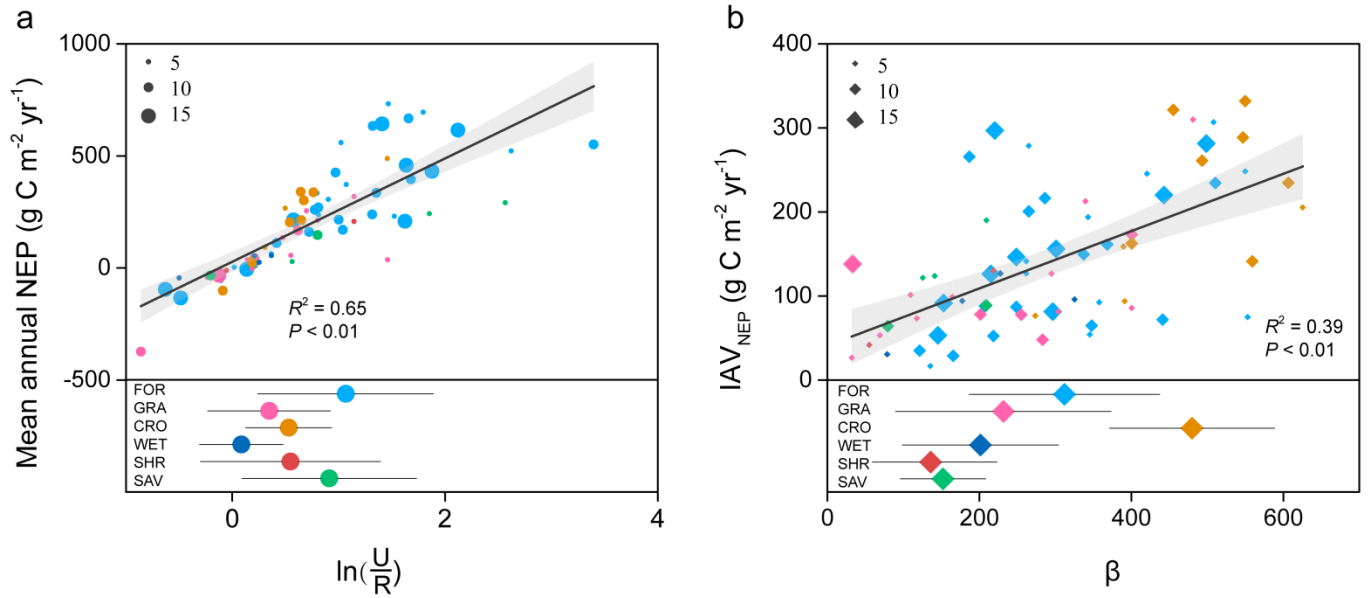


386

387 **Figure 2** Relationship between annual NEP and  $\frac{U}{R}$  for Jena Inversion product (of the form

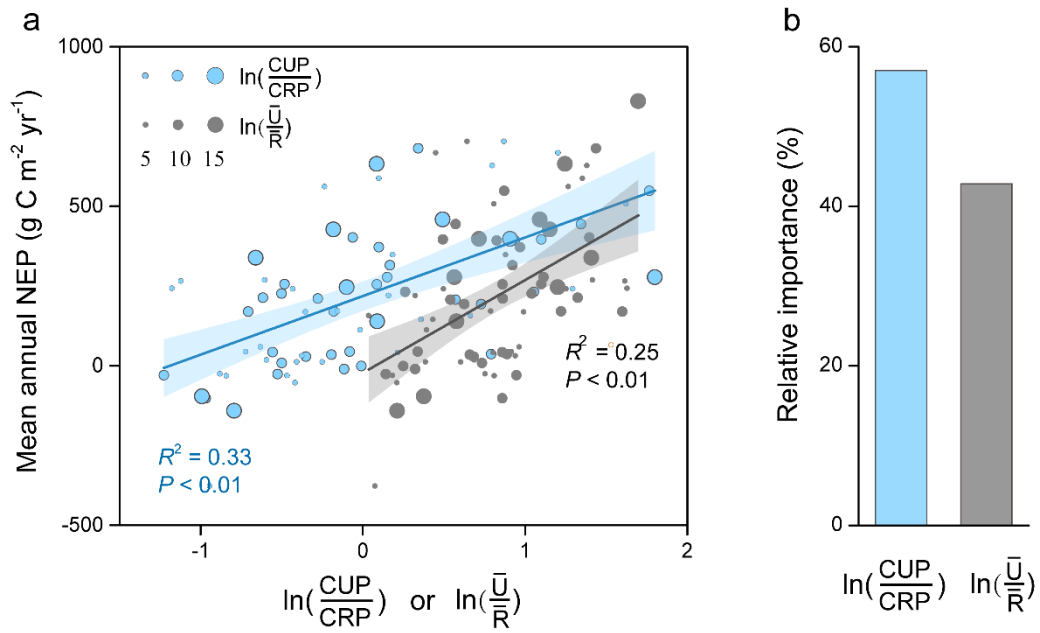
388  $NEP = \beta \cdot \ln\left(\frac{U}{R}\right)$ ). The black box indicates the location of the sample.

389

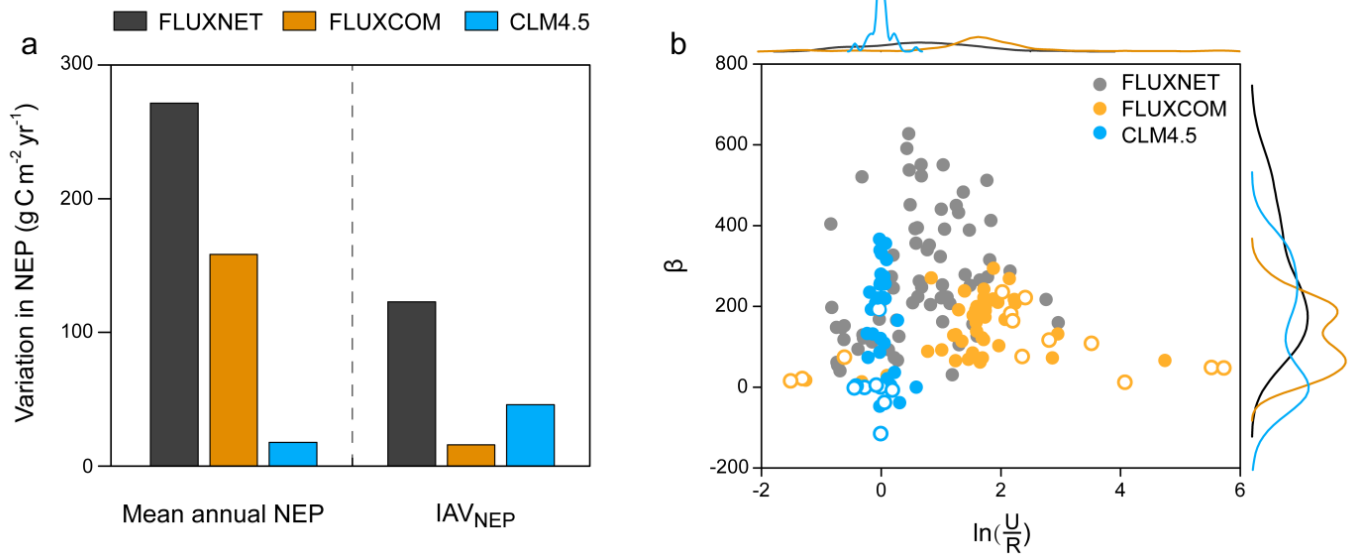


390  
 391 **Figure 3** Contributions of the two indicators in explaining the spatial patterns of mean annual  
 392 NEP and IAV<sub>NEP</sub>. **a**, The relationship between annual mean NEP and  $\ln(\frac{U}{R})$  across FLUXNET  
 393 sites ( $R^2 = 0.65$ ,  $P < 0.01$ ). The insets show the variation of  $\ln(\frac{U}{R})$  for different terrestrial  
 394 biomes. **b**, The explanation of  $\beta$  on IAV<sub>NEP</sub> ( $R^2 = 0.39$ ,  $P < 0.01$ ). The insets show the distribution  
 395 of parameter  $\beta$  for different terrestrial biomes. The number of site-years at each site is indicated  
 396 with the size of the point.

397



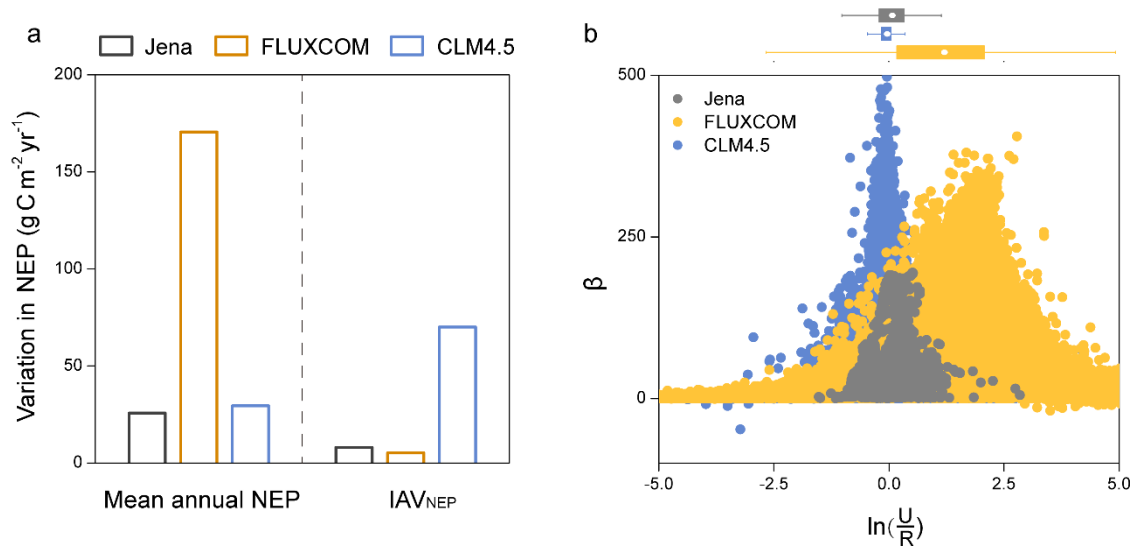
398  
 399 **Figure 4** The relative contributions of the local indicators in explaining the spatial patterns of  
 400 mean annual NEP. **a**, The linear regression between mean annual NEP with  $\frac{CUP}{CRP}$  ( $R^2 = 0.33$ ,  $P$   
 401  $< 0.01$ ) and  $\frac{\bar{U}}{\bar{R}}$  ( $R^2 = 0.25$ ,  $P < 0.01$ ) across sites. **b**, The relative contributions of each indicator  
 402 to the spatial variation of NEP. The number of site-years at each site is indicated with the size  
 403 of the point.  
 404



405

406 **Figure 5** Representations of the spatially varying NEP and its local indicators in FLUXCOM  
 407 product and the Community Land Model (CLM4.5) at the FLUXNET site level. **a**, The variation  
 408 of mean annual NEP and IAV<sub>NEP</sub> derives from FLUXNET, FLUXCOM and CLM4.5. Variation  
 409 in mean annual NEP: the standard deviation of mean annual NEP across sites; Variation in  
 410 IAV<sub>NEP</sub>: the standard deviation of IAV<sub>NEP</sub> across sites. **b**, Representations of the local indicators  
 411 for NEP in FLUXNET, FLUXCOM and CLM4.5. The corresponding distributions of  $\ln\left(\frac{U}{R}\right)$   
 412 and  $\beta$  are shown at the top and right. Significance of the relationship between annual NEP and  
 413  $\ln\left(\frac{U}{R}\right)$  for each site is indicated by the circle: closed circles:  $P < 0.05$ ; open circles:  $P > 0.05$ .  
 414 Note that the modeled results are from the pixels extracted from the same locations of the flux  
 415 tower sites.

416



417  
 418 **Figure 6** Representations of the spatially varying NEP and its local indicators in FLUXCOM  
 419 product and the Community Land Model (CLM4.5) at the global scale. a, The variation of mean  
 420 annual NEP and IAV<sub>NEP</sub> derives from Jena Inversion, FLUXCOM and CLM4.5. Variation in  
 421 mean annual NEP: the spatial variation of mean annual NEP; Variation in IAV<sub>NEP</sub>: the spatial  
 422 variation of standard deviation in IAV<sub>NEP</sub>. b, Representations of the local indicators for NEP in  
 423 Jena Inversion, FLUXCOM and CLM4.5.

424

## 425 **References**

- 426 Ahlström, A., Raupach, M. R., Schurgers, G., Smith, B., Arneeth, A., Jung, M., Reichstein, M.,  
427 Canadell, J. G., Friedlingstein, P., Jain, A. K., Kato, E., Poulter, B., Sitch, S., Stocker, B.  
428 D., Viovy, N., Wang, Y., Wiltshire, A., Zaehle, S., and Zeng, N.: The dominant role of semi-  
429 arid ecosystems in the trend and variability of the land CO<sub>2</sub> sink. *Science*, 348, 895-899,  
430 2015.
- 431 Arora, V. K., Katavouta, A., Williams, R. G., Jones, C. D., Brovkin, V., Friedlingstein, P.,  
432 Schwinger, J., Bopp, L., Boucher, O., Cadule, P., Chamberlain, M. A., Christian, J. R.,  
433 Delire, C., Fisher, R. A., Hajima, T., Ilyina, T., Joetzjer, E., Kawamiya, M., Koven, C.,  
434 Krasting, J., Law, R. M., Lawrence, D. M., Lenton, A., Lindsay, K., Pongratz, J., Raddatz,  
435 T., Séférian, R., Tachiiri, K., Tjiputra, J. F., Wiltshire, A., Wu, T., and Ziehn, T.: Carbon-  
436 concentration and carbon-climate feedbacks in CMIP6 models, and their comparison to  
437 CMIP5 models, *Biogeosciences Discuss.*, <https://doi.org/10.5194/bg-2019-473>, in review,  
438 2019.
- 439 Baldocchi, D., Chu, H., and Reichstein, M.: Inter-annual variability of net and gross ecosystem  
440 carbon fluxes: A review. *Agric. For. Meteorol.*, 249, 520-533, 2018.
- 441 Baldocchi, D., Sturtevant, C., and Contributors, F.: Does day and night sampling reduce spurious  
442 correlation between canopy photosynthesis and ecosystem respiration? *Agric. For.*  
443 *Meteorol.*, 207, 117-126, 2015.
- 444 Besnard, S., Carvalhais, N., Arain, A., Black, A., de Bruin, S., Buchmann, N., Cescatti, A., Chen,  
445 J., J.Clevers, J.G.P.W., Desai, A.R., Gough, C.M., Havrankova, K., Herold, M., Hörtnagl,  
446 L., Jung, M., Knohl, A., Kruijt, B., Krupkova, L., Law, B.E., Lindroth, A., Noormets, A.,  
447 Roupsard, O., Steinbrecher, R., Varlagin, A., Vincke, C. and Reichstein, M.: Quantifying  
448 the effect of forest age in annual net forest carbon balance. *Environ. Res. Lett.*, 13, 124018,  
449 2018.
- 450 Biederman, J. A., Scott, R. L., Goulden, M. L., Vargas, R., Litvak, M. E., Kolb, T. E., Yopez, E.  
451 A., Oechel, W. C., Blanken, P. D., Bell, T. W., Garatuza-Payan, J., Maurer, . E., Dore, S.,  
452 and Burns, S. P.: Terrestrial carbon balance in a drier world: the effects of water availability  
453 in southwestern North America. *Glob. Change Biol.*, 22, 1867-1879, 2016.
- 454 Bonan, G. B., Patton, E. G., Harman, I. N., Oleson, K. W., Finnigan, J. J., Lu, Y., and Burakowski,  
455 E. A.: Modeling canopy-induced turbulence in the Earth system: a unified parameterization  
456 of turbulent exchange within plant canopies and the roughness sublayer (CLM-ml v0).  
457 *Geosci. Model Dev.*, 11, 1467-1496, 2018.
- 458 Carpenter, S. R., and Brock, W. A.: Rising variance: a leading indicator of ecological transition.  
459 *Ecol. Lett.*, 9, 311-318, 2006.
- 460 Churkina, G., Schimel, D., Braswell, B. H., and Xiao, X.: Spatial analysis of growing season  
461 length control over net ecosystem exchange. *Glob. Change Biol.*, 11, 1777-1787, 2005.

462 Ciais, P., Tan, J., Wang, X., Roedenbeck, C., Chevallier, F., Piao, S. L., Moriarty, R., Broquet,  
463 G., Le Quéré, C., Canadell, J. G., Peng, S., Poulter, B., Liu Z., and Tans, P.: Five decades  
464 of northern land carbon uptake revealed by the interhemispheric CO<sub>2</sub> gradient. *Nature*, 568,  
465 221-225, 2019.

466 Cui, E., Huang, K., Arain, M. A., Fisher, J. B., Huntzinger, D. N., Ito, A., Luo, Y., Jain, A. K.,  
467 Mao, J., Michalak, A. M., Niu, S., Parazoo, N. C., Peng, C., Peng, S., Poulter, B., Ricciuto,  
468 D. M., Schaefer, K. M., Schwalm, C. R., Shi, X., Tian, H., Wang, W., Wang, J., Wei, Y.,  
469 Yan, E., Yan, L., Zeng, N., Zhu, Q., & Xia, J.: Vegetation functional properties determine  
470 uncertainty of simulated ecosystem productivity: A traceability analysis in the East Asian  
471 monsoon region. *Global Biogeochem. Cy.*, 33, 668-689, 2019.

472 Fu, Z., Dong, J., Zhou, Y., Stoy, P. C., and Niu, S.: Long term trend and interannual variability  
473 of land carbon uptake-the attribution and processes. *Environ. Res. Lett.*, 12, 014018, 2017.

474 Fu, Z., Stoy, P. C., Poulter, B., Gerken, T., Zhang, Z., Wakkulcho, G., and Niu, S.: Maximum  
475 carbon uptake rate dominates the interannual variability of global net ecosystem exchange.  
476 *Glob. Change Biol.*, 25, 3381-3394, 2019.

477 Gilmanov, T. G., Tieszen, L. L., Wylie, B. K., Flanagan, L. B., Frank, A. B., Haferkamp, M. R.,  
478 Meyers, T. P., and Morgan, J. A.: Integration of CO<sub>2</sub> flux and remotely-sensed data for  
479 primary production and ecosystem respiration analyses in the Northern Great Plains:  
480 Potential for quantitative spatial extrapolation. *Global Ecol. Biogeogr.*, 14, 271-292, 2005.

481 Gray, J. M., Frohling, S., Kort, E. A., Ray, D. K., Kucharik, C. J., Ramankutty, N., and Friedl,  
482 M. A.: Direct human influence on atmospheric CO<sub>2</sub> seasonality from increased cropland  
483 productivity. *Nature*, 515, 398-401, 2014.

484 Grömping, U.: Estimators of relative importance in linear regression based on variance  
485 decomposition. *Am. Stat.*, 61, 139-147, 2007.

486 Huang, K., Xia, J., Wang, Y., Ahlström, A., Chen, J., Cook, R. B., Cui, E., Fang, Y., Fisher, J. B.,  
487 Huntzinger, D. N., Li, Z., Michalak, A. M., Qiao, Y., Schaefer, K., Schwalm, C., Wang, J.,  
488 Wei, Y., Xu, X., Yan, L., Bian C., and Luo, Y.: Enhanced peak growth of global vegetation  
489 and its key mechanisms. *Nat. Ecol. Evol.*, 2, 1897-1905, 2018.

490 Jung, M., Reichstein, M., Schwalm, C. R., Huntingford, C., Sitch, S., Ahlström, A., Arneeth, A.,  
491 Camps-Valls, G., Ciais, P., Friedlingstein, P., Gans, F., Ichii, K., Jain, A. K., Kato, E., Papale,  
492 D., Poulter, B., Raduly, B., Rödenbeck, C., Tramontana, G., Viovy, N., Wang, Y., Weber,  
493 U., Zaehle S., and Zeng, N.: Compensatory water effects link yearly global land CO<sub>2</sub> sink  
494 changes to temperature. *Nature*, 541, 516-520, 2017.

495 Jung, M., Schwalm, C., Migliavacca, M., Walther, S., Camps-Valls, G., Koirala, S., Anthoni, P.,  
496 Besnard, S., Bodesheim, P., Carvalhais, N., Chevallier, F., Gans, F., Goll, D. S., Haverd, V.,  
497 Köhler, P., Ichii, K., Jain, A. K., Liu, J., Lombardozzi, D., Nabel, J. E. M. S., Nelson, J. A.,  
498 O'Sullivan, M., Pallandt, M., Papale, D., Peters, W., Pongratz, J., Rödenbeck, C., Sitch, S.,  
499 Tramontana, G., Walker, A., Weber, U., and Reichstein, M.: Scaling carbon fluxes from  
500 eddy covariance sites to globe: synthesis and evaluation of the FLUXCOM approach,

501 Biogeosciences, 17, 1343-1365, 2020.

502 Keenan, T. F., Gray, J., Friedl, M. A., Toomey, M., Bohrer, G., Hollinger, D. Y., Munger, J. W.,  
503 O’Keefe, J., Schmid, H. P., Wing, I. S., Yang, B., and Richardson, A. D.: Net carbon uptake  
504 has increased through warming-induced changes in temperate forest phenology. *Nat. Clim.*  
505 *Change*, 4, 598-604, 2014.

506 Kunstler, G., Falster, D., Coomes, D. A., Hui, F., Kooyman, R. M., Laughlin, D. C., Poorter, L.,  
507 Vanderwel, M., Vieilledent, G., Wright, S. J., Aiba, M., Baraloto, C., Caspersen, J.,  
508 Cornelissen, J. H. C., Gourlet-Fleury, S., Hanewinkel, M., Herault, B., Kattge, J.,  
509 Kurokawa, H., Onoda, Y., Peñuelas, J., Poorter, H., Uriarte, M., Richardson, S., Ruiz-  
510 Benito, P., Sun, I., Ståhl, G., Swenson, N. G., Thompson, J., Westerlund, B., Wirth, C.,  
511 Zavala, M. A., Zeng, H., Zimmerman, J. K., Zimmermann N. E., and Westoby, M.: Plant  
512 functional traits have globally consistent effects on competition. *Nature*, 529, 204-207,  
513 2016.

514 Le Quéré, C., Andrew, R. M., Friedlingstein, P., Sitch, S., Hauck, J., Pongratz, J., Pickers, P. A.,  
515 Korsbakken, J. I., Peters, G. P., Canadell, J. G., Arneeth, A., Arora, V. K., Barbero, L., Bastos,  
516 A., Bopp, L., Chevallier, F., Chini, L. P., Ciais, P., Doney, S. C., Gkritzalis, T., Goll, D. S.,  
517 Harris, I., Haverd, V., Hoffman, F. M., Hoppema, M., Houghton, R. A., Hurtt, G., Ilyina,  
518 T., Jain, A. K., Johannessen, T., Jones, C. D., Kato, E., Keeling, R. F., Goldewijk, K. K.,  
519 Landschützer, P., Lefèvre, N., Lienert, S., Liu, Z., Lombardozzi, D., Metzl, N., Munro, D.  
520 R., Nabel, J. E. M. S., Nakaoka, S., Neill, C., Olsen, A., Ono, T., Patra, P., Peregón, A.,  
521 Peters, W., Peylin, P., Pfeil, B., Pierrot, D., Poulter, B., Rehder, G., Resplandy, L.,  
522 Robertson, E., Rocher, M., Rödenbeck, C., Schuster, U., Schwinger, J., Séférian, R.,  
523 Skjelvan, I., Steinhoff, T., Sutton, A., Tans, P. P., Tian, H., Tilbrook, B., Tubiello, F. N., van  
524 der Laan-Luijkx, I. T., van der Werf, G. R., Viovy, N., Walker, A. P., Wiltshire, A. J., Wright,  
525 R., Zaehle, S., and Zheng, B.: Global carbon budget 2018. *Earth Syst. Sci. Data*, 10, 405,  
526 2018.

527 Li, G., Han, H., Du, Y., Hui, D., Xia, J., Niu, S., Li, X., and Wan, S.: Effects of warming and  
528 increased precipitation on net ecosystem productivity: a long-term manipulative  
529 experiment in a semiarid grassland. *Agric. For. Meteorol.*, 232, 359-366, 2017.

530 Luo, Y., and Weng, E.: Dynamic disequilibrium of the terrestrial carbon cycle under global  
531 change. *Trends Ecol. Evol.*, 26, 96-104, 2011.

532 Luo, Y., and Zhou, X.: *Soil respiration and the environment*. Elsevier, 2006.

533 Marcolla, B., Rödenbeck, C., and Cescatti, A.: Patterns and controls of inter-annual variability  
534 in the terrestrial carbon budget. *Biogeosciences*, 14, 3815-3829, 2017.

535 Musavi, T., Migliavacca, M., Reichstein, M., Kattge, J., Wirth, C., Black, T. A., Janssens, I.,  
536 Knohl, A., Loustau, D., Roupsard, O., Varlagin, A., Rambal, S., Cescatti, A., Gianelle, D.,  
537 Kondo, H., Tamrakar, R., and Mahecha, M. D.: Stand age and species richness dampen  
538 interannual variation of ecosystem-level photosynthetic capacity. *Nat. Ecol. Evol.*, 1, 0048,  
539 2017.



540 Niu, S., Fu, Z., Luo, Y., Stoy, P. C., Keenan, T. F., Poulter, B., Zhang, L., Piao, S., Zhou, X.,  
541 Zheng, H., Han, J., Wang, Q., and Yu, G.: Interannual variability of ecosystem carbon  
542 exchange: From observation to prediction. *Global Ecol. Biogeogr.*, 26, 1225-1237, 2017.

543 Novick, K. A., Oishi, A. C., Ward, E. J., Siqueira, M. B., Juang, J. Y., and Stoy, P. C.: On the  
544 difference in the net ecosystem exchange of CO<sub>2</sub> between deciduous and evergreen forests  
545 in the southeastern United States. *Glob. Change Biol.*, 21, 827-842, 2015.

546 Oleson, K. W., Lawrence, D. M., Bonan, G. B., Drewniak, B., Huang, M., Koven, C. D., Levis,  
547 S., Li, F., Riley, W. J., Subin, Z. M., Swenson, S. C., Thornton, P. E., Bozbiyik, A., Fisher,  
548 R., Heald, C. L., Kluzek, E., Lamarque, J.-F., Lawrence, P. J., Leung, L. R., Lipscomb, W.,  
549 Muszala, S., Ricciuto, D. M., Sacks, W., Sun, Y., Tang, J., and Yang, Z.-L.: Technical  
550 description of version 4.5 of the Community Land Model (CLM), NCAR Earth System  
551 Laboratory-Climate and Global Dynamics Division, Boulder, Colorado, USA, Tech. Rep.  
552 TN-503+STR, [http://www.cesm.ucar.edu/models/cesm1.2/clm/CLM45\\_Tech\\_Note.pdf](http://www.cesm.ucar.edu/models/cesm1.2/clm/CLM45_Tech_Note.pdf)  
553 (last access: 27 September 2017), 2013.

554 Pastorello, G., Papale, D., Chu, H., Trotta, C., Agarwal, D., Canfora, E., Baldocchi, D., and Torn,  
555 M.: A new data set to keep a sharper eye on land-air exchanges. *Eos*, 98, 2017.

556 Peng, S., Ciais, P., Chevallier, F., Peylin, P., Cadule, P., Sitch, S., Piao, S., Ahlström, A.,  
557 Huntingford, C., Levy, P., Li, X., Liu, Y., Lomas, M., Poulter, B., Viovy, N., Wang, T.,  
558 Wang, X., Zaehle, S., Zeng, N., Zhao, F., and Zhao, H.: Benchmarking the seasonal cycle  
559 of CO<sub>2</sub> fluxes simulated by terrestrial ecosystem models. *Global Biogeochem. Cy.*, 29, 46-  
560 64, 2015.

561 Peylin, P., Law, R. M., Gurney, K. R., Chevallier, F., Jacobson, A. R., Maki, T., Niwa, Y., Patra,  
562 P. K., Peters, W., Rayner, P. J., Rödenbeck, C., van der Laan-Luijkx, I. T., and Zhang, X.:  
563 Global atmospheric carbon budget: results from an ensemble of atmospheric CO<sub>2</sub>  
564 inversions. *Biogeosciences*, 10, 6699-6720, 2013.

565 Poulter, B., Frank, D., Ciais, P., Myneni, R. B., Andela, N., Bi, J., Broquet, G., Canadell, J. G.,  
566 Chevallier, F., Liu, Y. Y., Running, S. W., Sitch, S., and van der Werf, G. R.: Contribution  
567 of semi-arid ecosystems to interannual variability of the global carbon cycle. *Nature*, 509,  
568 600-603, 2014.

569 Randerson, J. T.: Climate science: Global warming and tropical carbon. *Nature*, 494, 319-320,  
570 2013.

571 Randerson, J. T., Chapin III, F. S., Harden, J. W., Neff, J. C., and Harmon, M. E.: Net ecosystem  
572 production: a comprehensive measure of net carbon accumulation by ecosystems. *Ecol.*  
573 *Appl.*, 12, 937-947, 2002.

574 R Development Core Team.: R: A Language and Environment for Statistical Computing 3-  
575 900051-07-0, R Foundation for Statistical Computing, Vienna, Austria, 2011.

576 Reichstein, M., Bahn, M., Mahecha, M. D., Kattge, J., and Baldocchi, D. D.: Linking plant and  
577 ecosystem functional biogeography. *Proc. Natl Acad. Sci. USA*, 111, 13697-13702, 2014.

578 Reichstein, M., Falge, E., Baldocchi, D., Papale, D., Aubinet, M., Berbigier, P., Bernhofer, C.,

579 Buchmann, N., Gilmanov, T., Granier, A., Grünwald, T., Havránková, K., Ilvesniemi, H.,  
580 Janous, D., Knohl, A., Laurila, T., Lohila, A., Loustau, D., Matteucci, G., Meyers, T.,  
581 Miglietta, F., Ourcival, J., Pumpanen J., Rambal, S., Rotenberg, E., Sanz, M., Tenhunen,  
582 J., Seufert, G., Vaccari, F., Vesala, T., Yakir, D., and Valentini, R.: On the separation of net  
583 ecosystem exchange into assimilation and ecosystem respiration: review and improved  
584 algorithm. *Glob. Change Biol.*, 11, 1424-1439, 2005.

585 Richardson, A. D., Keenan, T. F., Migliavacca, M., Ryu, Y., Sonnentag, O., and Toomey, M.:  
586 Climate change, phenology, and phenological control of vegetation feedbacks to the  
587 climate system. *Agric. For. Meteorol.*, 169, 156-173, 2013.

588 Rödenbeck, C., Zaehle, S., Keeling, R., and Heimann, M.: How does the terrestrial carbon  
589 exchange respond to inter-annual climatic variations? *Biogeosciences*, 15, 2481-2498,  
590 2018.

591 Sakschewski, B., von Bloh, W., Boit, A., Rammig, A., Kattge, J., Poorter, L., Peñuelas, J., and  
592 Thonicke, K.: Leaf and stem economics spectra drive diversity of functional plant traits in  
593 a dynamic global vegetation model. *Glob. Change Biol.*, 21, 2711-2725, 2015.

594 Scheffer, M., Bascompte, J., Brock, W. A., Brovkin, V., Carpenter, S. R., Dakos, V., Held, H.,  
595 van Nes, E. H., Rietkerk, M., and Sugihara, G.: Early-warning signals for critical transitions.  
596 *Nature*, 461, 53-59, 2009.

597 Valentini, R., Matteucci, G., Dolman, A. J., Schulze, E. D., Rebmann, C. J. M. E. A. G., Moors,  
598 E. J., Granier, A., Gross, P., Jensen, N. O., Pilegaard, K., Lindroth, A., Grelle, A., Bernhofer,  
599 C., Grünwald, T., Aubinet, M., Ceulemans, R., Kowalski, A. S., Vesala, T., Rannik, Ü.,  
600 Berbigier, P., Loustau, D., Guðmundsson, J., Thorgeirsson, H., Ibrom, A., Morgenstern, K.,  
601 Clement, R., Moncrieff, J., Montagnani, L., Minerbi S., and Jarvis, P. G.: Respiration as  
602 the main determinant of carbon balance in European forests. *Nature*, 404, 861-865, 2000.

603 Von Buttlar, J., Zscheischler, J., Rammig, A., Sippel, S., Reichstein, M., Knohl, A., Jung, M.,  
604 Menzer, O., Arain, M., Buchmann, N., Cescatti, A., Geinelle, D., Kiely, G., Law, B.,  
605 Magliudo, V., Margolis, H., McCaughey, H., Merbold, L., Migliavacca, M., Montagnani,  
606 L., Oechel, W., Pavelka, M., Pelchl, M., Rambal, S., Raschi, A., Scott, R.L., Vaccari, F.,  
607 Van Gorsel, E., Varlagin, A., Wohlfahrt, G., and Mahecha, M.: Impacts of droughts and  
608 extreme temperature events on gross primary production and ecosystem respiration: a  
609 systematic assessment across ecosystems and climate zones. *Biogeosciences*, 15, 1293-  
610 1318, 2017.

611 Xia, J., Chen, J., Piao, S., Ciais, P., Luo, Y., and Wan, S.: Terrestrial carbon cycle affected by  
612 non-uniform climate warming. *Nat. Geosci.*, 7, 173-180, 2014.

613 Xia, J., McGuire, A. D., Lawrence, D., Burke, E., Chen, G., Chen, X., Delire, C., Koven, C.,  
614 MacDougall, A., Peng, S., Rinke, A., Saito, K., Zhang, W., Alkama, R., Bohn, T. J., Ciais,  
615 P., Decharme, B., Gouttevin, I., Hajima, T., Hayes, D. J., Huang, K., Ji, D., Krinner, G.,  
616 Lettenmaier, D. P., Miller, P. A., Moore, J. C., Smith, B., Sueyoshi, T., Shi, Z., Yan, L.,  
617 Liang, J., Jiang, L., Zhang, Q., and Luo, Y.: Terrestrial ecosystem model performance in

618           simulating productivity and its vulnerability to climate change in the northern permafrost  
619           region. *J. Geophys. Res-Bioge.*, 122, 430-446, 2017.

620 Xia, J., Niu, S., Ciais, P., Janssens, I. A., Chen, J., Ammann, C., Arain, A., Blanken, P. D.,  
621           Cescatti, A., Bonal, D., Buchmann, N., Curtis, P. S., Chen, S., Dong, J., Flanagan, L. B.,  
622           Frankenberg, C., Georgiadis, T., Gough, C. M., Hui, D., Kiely, G., Li, J., Lund, M.,  
623           Magliulo, V., Marcolla, B., Merbold, L., Montagnani, L., Moors, E. J., Olesen, J. E., Piao,  
624           S., Raschi, A., Rouspard, O., Suyker, A. E., Urbaniak, M., Vaccari, F. P., Varlagin, A.,  
625           Vesala, T., Wilkinson, M., Weng, E., Wohlfahrt, G., Yan, L., and Luo, Y.: Joint control of  
626           terrestrial gross primary productivity by plant phenology and physiology. *Proc. Natl Acad.*  
627           *Sci. USA*, 112, 2788-2793, 2015.

628 Xia, J., Wang, J., and Niu, S.: Research challenges and opportunities for using big data in global  
629           change biology. *Glob. Change Biol.*, 2020. <https://doi.org/10.1111/gcb.15317>

630 Yu, G., Chen, Z., Piao, S., Peng, C., Ciais, P., Wang, Q., Li, X., and Zhu, X.: High carbon dioxide  
631           uptake by subtropical forest ecosystems in the East Asian monsoon region. *Proc. Natl Acad.*  
632           *Sci. USA*, 111, 4910-4915, 2014.

633 Zeng, N., Zhao, F., Collatz, G. J., Kalnay, E., Salawitch, R. J., West, T. O., and Guanter, L.:  
634           Agricultural Green Revolution as a driver of increasing atmospheric CO<sub>2</sub> seasonal  
635           amplitude. *Nature*, 515, 394-397, 2014.

636 Zhao, J., Peichl, M., Öquist, M., and Nilsson, M. B.: Gross primary production controls the  
637           subsequent winter CO<sub>2</sub> exchange in a boreal peatland. *Glob. Change Biol.*, 22, 4028-4037,  
638           2016.

639 Zhou, S., Zhang, Y., Ciais, P., Xiao, X., Luo, Y., Caylor, K. K., Huang, Y., and Wang, G.:  
640           Dominant role of plant physiology in trend and variability of gross primary productivity in  
641           North America. *Sci. Rep.*, 7, 41366, 2017.

642